European Journal of Orthodontics 20 (1998) 79–92

Surface roughness of orthodontic wires via atomic force microscopy, laser specular reflectance, and profilometry

Christoph Bourauel*, Thomas Fries**, Dieter Drescher* and Reinhard Plietsch***

*Department of Orthodontics, University of Bonn, **Fries Research and Technology GmbH, Bergisch Gladbach and ***Forschungszentrum Karlsruhe, Germany

SUMMARY The surface roughness of orthodontic archwires is an essential factor that determines the effectiveness of arch-guided tooth movement. Using the non-destructive techniques of atomic force microscopy (AFM) and of laser specular reflectance, the surface roughness of 11 nickel-titanium orthodontic wires, a stainless steel and a β-titanium wire was measured. The results were compared with those obtained using surface profilometry. The smoothest wire, stainless steel, had an optical roughness of 0.10 μm, compared with 0.09 μm from AFM and 0.06 from profilometry. The surface roughness for the β-titanium wire measured by all three methods was approximately 0.21 μm, while that of the NiTi wires ranged from 0.10 to 1.30 μm. As the surface roughness not only affects the effectiveness of sliding mechanics, but also the corrosion behaviour and the aesthetics of orthodontic components, the manufacturers of orthodontic wires should make an effort to improve the surface quality of their products.

Introduction

Dental materials have to withstand mechanical, thermal, and chemical stresses in the patient's mouth and must have a sufficient biocompatibility in this aggressive environment. Consequently, the surface quality, i.e. the surface roughness of dental materials is of utmost importance, as this determines the area of the contact surface and thus influences the corrosion behaviour and the biocompatibility (Kappert *et al.*, 1988).

In orthodontics, surface roughness of orthodontic archwires additionally may affect the aesthetics of the appliance and the perfomance of sliding mechanics by its influence on the coefficient of friction. Guiding a tooth along an archwire results in tipping and rotating of the tooth and in a contact between the bracket and the guiding wire (Figure 1). Consequently, frictional forces may reduce the orthodontic force by 50 per cent or more (Drescher *et al.*, 1989). The loss due to friction depends on a large number of mechanical parameters of the combination of archwires and brackets being used, but above all the material parameters of the guiding archwire are dominant factors. Frictional losses in orthodontic force are reported to be lowest when stainless steel wires are employed and increase in

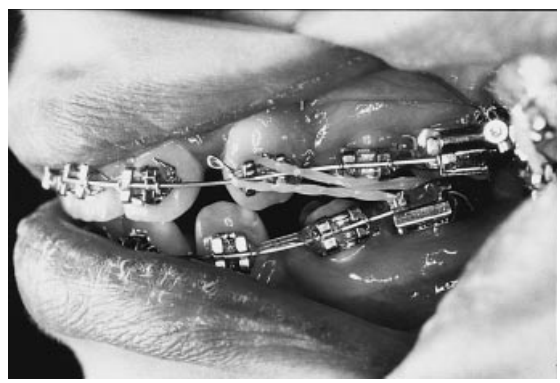

Figure 1 An example of sliding mechanics. Because the canine tends to tip in the desired direction of tooth movement, friction between the bracket and the archwire results in an S-shaped bending of the guiding arch and in significant loss of orthodontic force.

the following order: cobalt-chrome alloys, nickel-titanium alloys, and β-titanium (Peterson *et al.*, 1982; Garner *et al.*, 1986; Drescher *et al.*, 1989; Kusy and Whitley, 1989; Kusy *et al.*, 1991; Keith *et al.*, 1994). This order coincides, in part, with the surface roughness of the archwires used, although the relationships between all the material parameters and the coefficient of friction together with their interactions are still not well known (e.g. Kusy *et al.*, 1988).

The principal technique for determining surface roughness is surface profilometry, in which a fine stylus is used to scan the topography in a single line of a preselected area. Drawbacks of this method are that surface defects adjacent to the scanning line are not measured and so these defects do not contribute to the overall measured surface roughness, and the invasive character of this technique which may damage the surface while scanning it.

Non-destructive, non-invasive alternatives based on optical methods (Vorburger and Teague, 1981) and on recently developed Scanning Tunnelling Microscopy (STM) (Binnig *et al.*, 1982) have been available for some time. With these methods it is possible to perform a surface analysis over preselected areas of a specimen without interacting directly with it. The optical methods include ellipsometry (Vedam and So, 1972), interferometry (Bennett, 1976), speckle-interferometry (Crane, 1970; Sprague, 1972; Léger *et al.*, 1975; Fujii *et al.*, 1976) and angular scattering distributions (Bennett and Porteus, 1961; Hensler, 1972; Holzer and Sung, 1976; Tanner, 1976, 1979; Tanner and Fahoum, 1976; Elson and Bennett, 1979). The simplest and fastest of these optical methods is laser specular reflectance (Hensler, 1972; Kusy *et al.*, 1988).

Scanning probe microscopy (SPM) includes different types of STMs (Kuk and Siverman, 1989), atomic force microsopy (AFM; Binnig *et al.*, 1986) and magnetic force microscopy (MFM; Wickramasinghe, 1990). Among these, AFM seems to be most suitable for the investigation of surface topography, as it offers the greatest variability in defining measuring areas.

This study focuses on the surface roughness of orthodontic archwires with an emphasis placed on those made from nickel-titanium. The three methods used, i.e. atomic force microscopy, laser specular reflectance, and surface profilometry are compared, and the surface roughness of the orthodontic archwires investigated is discussed in relation to the generated frictional losses measured for these wires in arch-guided tooth movement in former studies.

Materials and methods

Orthodontic nickel-titanium alloys

Nickel-titanium alloys, first described by Buehler *et al.*, in 1963, have been widely used in orthodontics for more than 20 years. These alloys have a composition of approximately 52 per cent nickel and 48 per cent titanium, resulting in properties such as shape memory effect and super-elasticity. A first use hypothesis for these wires was given by Andreasen and Brady (1972), and their application in orthodontic treatment has increased rapidly since then. Eleven commercial nickel-titanium wires were selected with the aim of characterizing their surface properties. For the purpose of comparison a stainless steel wire and a β-titanium wire were included in this study. Tables 1 and 2 list all products investigated together with the manufacturers, the wire cross-sections, their chemical composition, and a short code for identification in the presentation of the results.

As the methods used for this study are inappropriate tools for the analysis of rounded surfaces, wires with a rectangular or quadratic cross-section were investigated, with the assumption that all wires of the same manufacturer undergo similar finishing processes (Kusy *et al.*, 1988). A validation of this assumption should be possible by measuring the product GAC Sentalloy (short code SSA) with multiple cross-sections (0.018 × 0.025-inch, 0.017 × 0.025-inch, 0.016 × 0.022-inch). The wire Neo-Sentalloy (code NSA) was available with three different tempers: F100, F200, F300. All three tempers were investigated with identical cross-sections. Two batches of all other wires were investigated using AFM, specular reflectance and profilometry, with the exception of Super Nitane and Orthonol wires, which were samples, the latter

Table 1 Orthodontic wires used in this study (chemical composition given in atomic per cent by the manufacturer (1) and by Thier (2) (personal communication, 1991).

Abbreviation	Manufacturer	Product	Wire cross-section	Chemical composition
AOT1/2	American Orthodontics	Memorywire NiTi	0.016″ × 0.022″	52.0% Ni(2) 48.0% Ti
DNT1/2	Dentaurum	Rematitan Lite	0.016″ × 0.022″	53.5% Ni(2) 46.5% Ti
FTS1/2	Forestadent	Titanol Superelastic	0.016″ × 0.022″	53.0% Ni(2) 47.0% Ti
HIT1/2	Unitek	Hi-T Steel	0.016″ × 0.022″	~72.0% Fe(1) ~18.0% Cr 8.0% Ni
NIS1/2	Unitek	Nitinol SE	0.016″ × 0.022″	52.8% Ni(2) 47.2% Ti
NIT1/2	Unitek	Nitinol	0.016″ × 0.022″	52.0% Ni(1) 45.0% Ti 3.0% Cr
NSA1 NSA2 NSA3	GAC	Neo Sentalloy F100 F200 F300	0.018″ × 0.025″	52.9% Ni(2) 47.1% Ti
ONI1/2	Ormco	NiTi	0.016″ × 0.022″	52.4% Ni(2) 47.6% Ti
OSN1	Ormco	Super Nitane	0.016″ × 0.022″	51.3% Ni(2) 48.7% Ti
RMO1/2	Rocky Mountain	Orthonol	0.016″ × 0.016″	51.8% Ni(2) 48.2% Ti
RMT1/2	Dentaurum	Rematitan	0.016″ × 0.022″	53.2% Ni(2) 46.8% Ti
SSA1 SSA2 SSA3	GAC	Sentalloy	0.018″ × 0.025″ 0.017″ × 0.025″ 0.016″ × 0.022″	52.6% Ni (2) 47.4% Ti
TMA1/2	Ormco	TMA	0.016″ × 0.022″	78.0% Ti(1) 11.0% Mo 6.0% Zr 4.0% Sn

Table 2 List of manufacturers of the wires investigated.

Manufacturer	
American Orthodontics	American Orthodontics, 1714 Cambridge Avenue, Sheboygan, WI 53082, USA
Dentaurum	Dentaurum, J.P. Winkelstroeter KG, Box 440, 75104 Pforzheim, Germany
Forestadent	Forestadent, Bernhard Förster GmbH, Box 660, 75106 Pforzheim, Germany
GAC	GAC International, Inc., 185 Oval Drive, Central Islip, NY 11722, USA
Ormco	ORMCO Corp., 1332 South Lone Hill Avenue, Glendora, CA 91740, USA
Rocky Mountain	RMO, PO Box 17085, Denver, CO 80217, USA
Unitek	3M Unitek, 2724 South Peck Road, Monrovia, CA 91016, USA

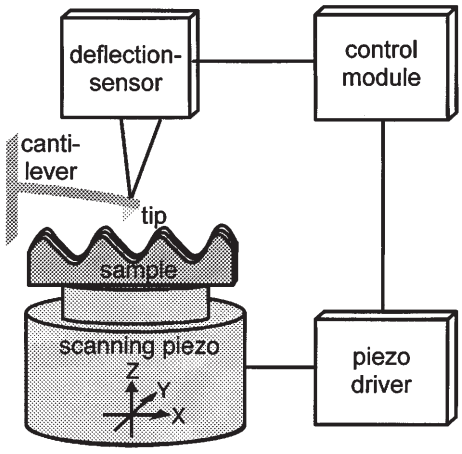

Figure 2 Principle of atomic force microscopy. The cantilever-mounted fine tip is brought near to the surface and, as the sample is moved by the piezo scanner interactions, produces vertical deflections which are registered by the deflection sensor.

having a cross-section of 0.016 × 0.016-inch. The surface of this cross-section could not accommodate the full beam width of the laser and, consequently, it was subjected only to AFM and profilometry measurements.

Atomic force microscopy

Figure 2 displays the principle of atomic force microscopy. The specimen was fixed to a scanning piezo with three translatory degrees of freedom. A very fine tip (radius <100 nm) served as a probe scanning the surface of the specimen. This tip was mounted on a thin cantilever of approximately 100 µm in length, having a deflection modulus between 0.001 and 100 N/m. Bringing the tip into a distance of about 10–100 nm of the specimen surface results in forces between 10^{-11} N and 10^{-6} N. This range of forces characterizes the interaction between the surface and the tip. Due to this interaction, the cantilever was bent and the vertical deflection of its end registered by a deflection sensor.

The generation of a surface scan was undertaken as follows: the scanning piezo moved the specimen in consecutive lines underneath the tip so that a preselected area of the surface was scanned in the XY-plane. At the same time, the scanning piezo was driven vertically to maintain the interaction, i.e. the force between the surface and the tip, at a constant level. Deviation from a predefined deflection of the cantilever generated a signal in the control module and this was fed into the piezo driver via a feedback loop. The vertical position of the scanning piezo thus provided information on the surface structure of the specimen.

A commercial AFM (Nanoscope III, Digital Instruments Inc., Santa Barbara, CA 93103) was used to perform the surface analysis of the orthodontic wires. Scanning areas of the apparatus may be from the atomic level up to 125 µm^2 with a maximum lateral and vertical resolution of 3–5 and 0.1 nm, respectively. The instrument was provided with the ability to both analyse the data and to display it in three dimensions. For the purpose of comparison, the root mean square roughness (RMS roughness, denoted as $R_{a,A}$ in the following) was chosen to characterize the topography of the orthodontic wires. For each wire three surface scans were taken with an area of 100 µm square, one in the middle of the wire and one at each end. The RMS roughness of these surface areas was determined and the mean and standard deviation were calculated from these values.

Laser specular reflectance

The set up used for laser specular reflectance was similar to that developed by Kusy and coworkers. They designed a manually operated spectrometer to investigate surface textures of different dental materials (Konishi *et al.*, 1985; Kusy and Whitley, 1985; Buckthal and Kusy, 1988; Haywood *et al.*, 1988; Kusy *et al.*, 1988; Mayhew and Kusy, 1988). Figure 3 is a schematic diagram of the experimental set up developed for this investigation: The wire, S, was mounted on a rotary table driven by a stepping motor. A focused beam of red laser light (wavelength λ = 632.8 nm, diameter 0.55 mm) from a 0.5-mW helium-neon laser (05 LLP 805, Darmstadt, Germany) impinged on the surface of the specimen at an angle α from the perpendicular. A small portion of the beam was split off and was measured by a photo-detector (D_R) to serve as a

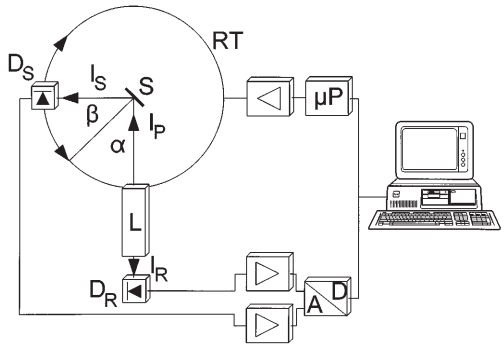

Figure 3 Schematic diagram of the experimental set up for laser specular reflectance. S = sample, RT = stepping motor driven rotary tables, L = HeNe-laser, I_R = reference beam, I_P = probe beam with an angle of incidence α, I_S = intensity of the beam reflected by the sample under an angle of β, D_R and D_S = detectors for the reference intensity and for the reflected intensity, μP = microprocessor board driving the rotary stages, A/D = analog/digital-conversion board.

reference of the incident intensity. The main part of the beam was reflected from the surface and its intensity was measured by a second detector (D_S) which was mounted on a second rotary table driven by its own stepping motor. The signals from the photo-detectors were amplified and fed via an analog/digital converter to a computer which controlled the stepping motors, and thus the angle of incidence, α, and the position of D_S.

If the surface of the wire was perfectly smooth, only specular reflectance would occur and the photo-detector would measure a reflected intensity only at an angle of reflection β = α. Each deviation from this law of reflection coincides with imperfections of the surface. Given a surface with a roughness of the same order of magnitude as the laser light impinging on it, diffuse reflection around the angle β can be measured with the detector D_R by rotating the second table about plus or minus 5 degrees around the angle of direct reflection. To ensure a good angular resolution, an aperture with a diameter of 1.0 mm was placed in front of the detector.

Measuring the spectra of reflected intensity for different values α, the optical RMS roughness (σ_O) of the wire surface can be determined from a formula presented by Tanner and Fahoum (1976):

$$\frac{I_s}{I_p} = \exp\left[-\left(\frac{4\pi\sigma_o}{\lambda}\right)^2 \cdot \cos^2\alpha\right], \qquad (1)$$

where I_S is the maximum reflected intensity at the angle of direct reflection β = α and I_P is the intensity of the probe beam. From this the average optical roughness $R_{a,O}$ can be calculated using the general relationship for stylus instruments (Vidosic, 1964):

$$R_{a,O} = \frac{\sigma_O}{1.11} \qquad (2)$$

Important restrictions with this method are the fact that only surfaces with a roughness $\sigma_O < \lambda$ can be measured and that the surface topography should approximate a Gaussian profile (Bennett and Porteus, 1961; Vorburger and Teague, 1981). These presuppositions limit measurements of the reflected intensity only at grazing incidence, i.e. for angles $\alpha \geq 76$ degrees, and to measurements of relatively smooth surfaces, i.e. those with an optical roughness of $\sigma_O \leq 0.2$ μm (Whitley *et al.*, 1987).

Laser spectra were generated for the following: all even numbered angles of incidence between 70 and 84 degrees, and one at 45 degrees. At the latter angle the reflected intensity was observed on a translucent screen. Five laser spectra were taken at each angle and the mean of the maximum relative reflected intensity I_S/I_P at β = α was calculated. Plotting the log of these values versus the cosine squared of the angle of incidence α, σ_O can be calculated according to formula (1). A linear regression analysis was performed with the data (PlotIt for Windows 3.02, Scientific Programming Enterprises, Haslett, MI 48840, USA) to determine the slopes of the lines and from these values the average optical roughness $R_{a,O}$ was calculated according to formula (2).

Surface profilometry

The surface profilometric studies were performed using a commercial profilometer (Hommel T 20,

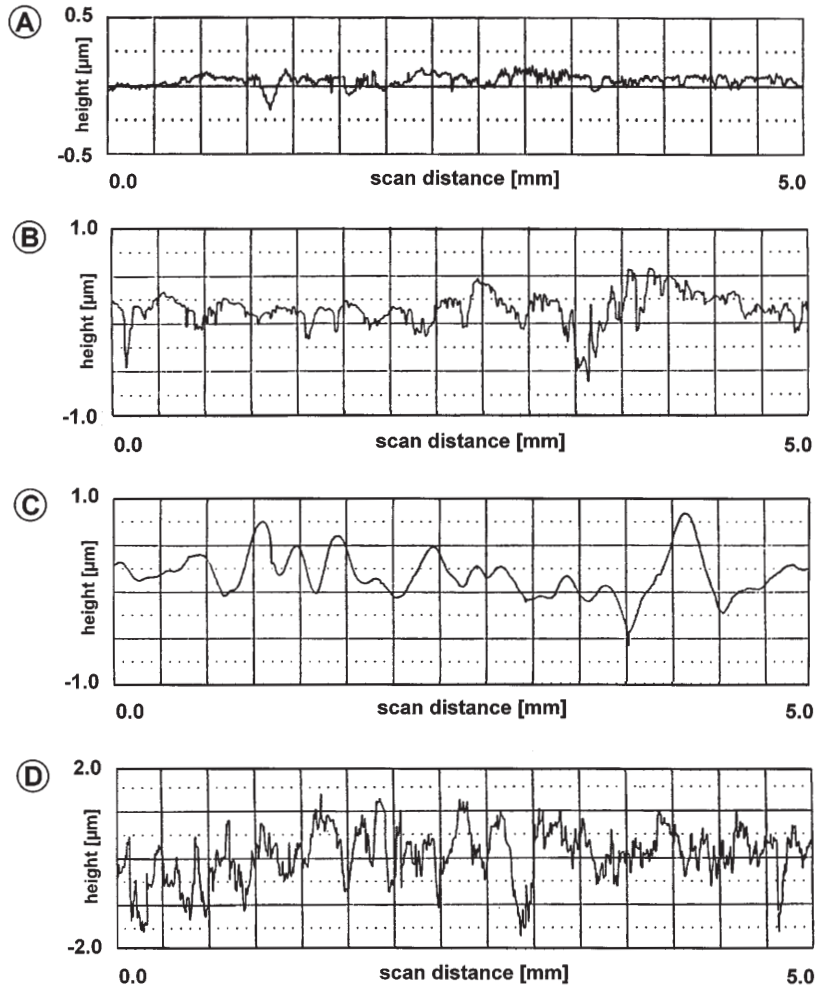

Figure 4 Typical profilometric scans of the orthodontic wires (a) stainless steel (HIT), (b) β-titanium (TMA), (c) nickel-titanium (RMT), and (d) NIT.

Hommel GmbH, Villingen-Schwenningen, Germany). This was equipped with a diamond tip having a radius of 5 µm and sensitive to vertical movements to an accuracy of ± 0.01 µm. The scanning distance was 5.0 mm each, and the equipment determined automatically the profilometric mean roughness R_a from the surface profile. Three profilometric scans were taken at different positions on the wire surface, and the mean and the standard deviation were calculated.

Results

Figure 4a–d depict the examples of profilometric scans of the wires HIT, TMA, RMT, and NIT. The scans reflect the typical surface structure of these wires. The stainless steel, HIT, one of the smoothest wires investigated, had a roughness with a short wavelength and a small amplitude (Figure 4a), whereas the β-titanium wire, TMA (Figure 4b), had a roughness with a distinctly

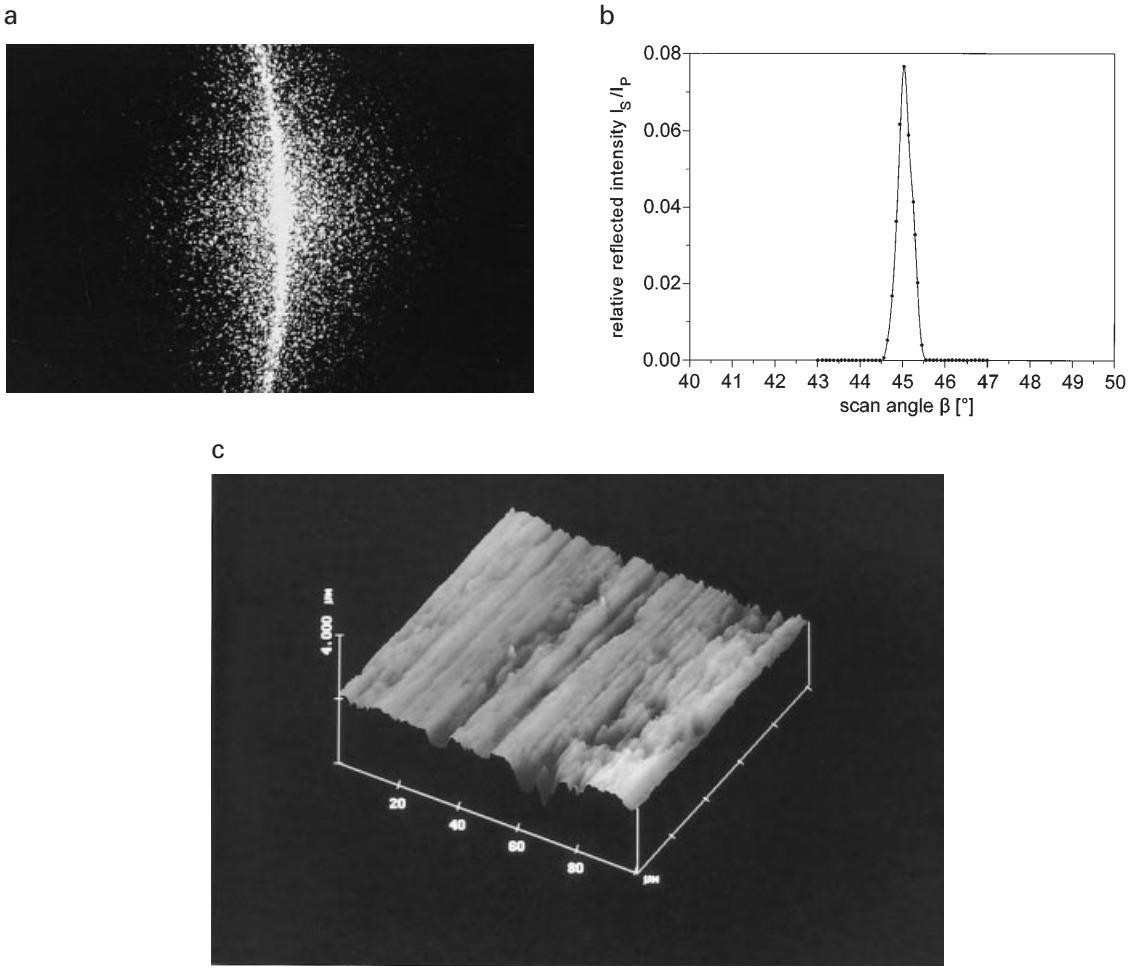

Figure 5 (a) Photograph of the reflected intensity of the stainless steel wire (HIT) at an angle of incidence of 45 degrees. Diffuse reflection surrounds a narrow peak with direct reflection. (b) Scanned distribution of the reflected intensity I_s at an angle of incidence of $\alpha = 45$ degrees. (c) A surface scan of 100×100 µm taken by the AFM.

higher amplitude at a comparable wavelength. The profilometric scans of the two nickel-titanium alloys, RMT (Figure 4c) and NIT (Figure 4d), illustrate the influence of different finishing processes of these wires. RMT had a surface texture with a long wavelength roughness at medium amplitude, whereas NIT had a high amplitude/short wavelength roughness.

Figures 5–8 summarize the results of the optical and the atomic force microscopy (AFM) measurements for the same wires. In each case (a) is a photograph of the speckle pattern at an angle of incidence of $\alpha = 45$ degrees taken from the translucent screen and (b) is the corresponding scanned distribution of the reflected intensity at the same angle of incidence. The AFM scans for these wires are depicted in Figures 5c–8c. The optical, as well as the AFM measurements underline the qualitative results derived from the profilometric measurements. The bright central

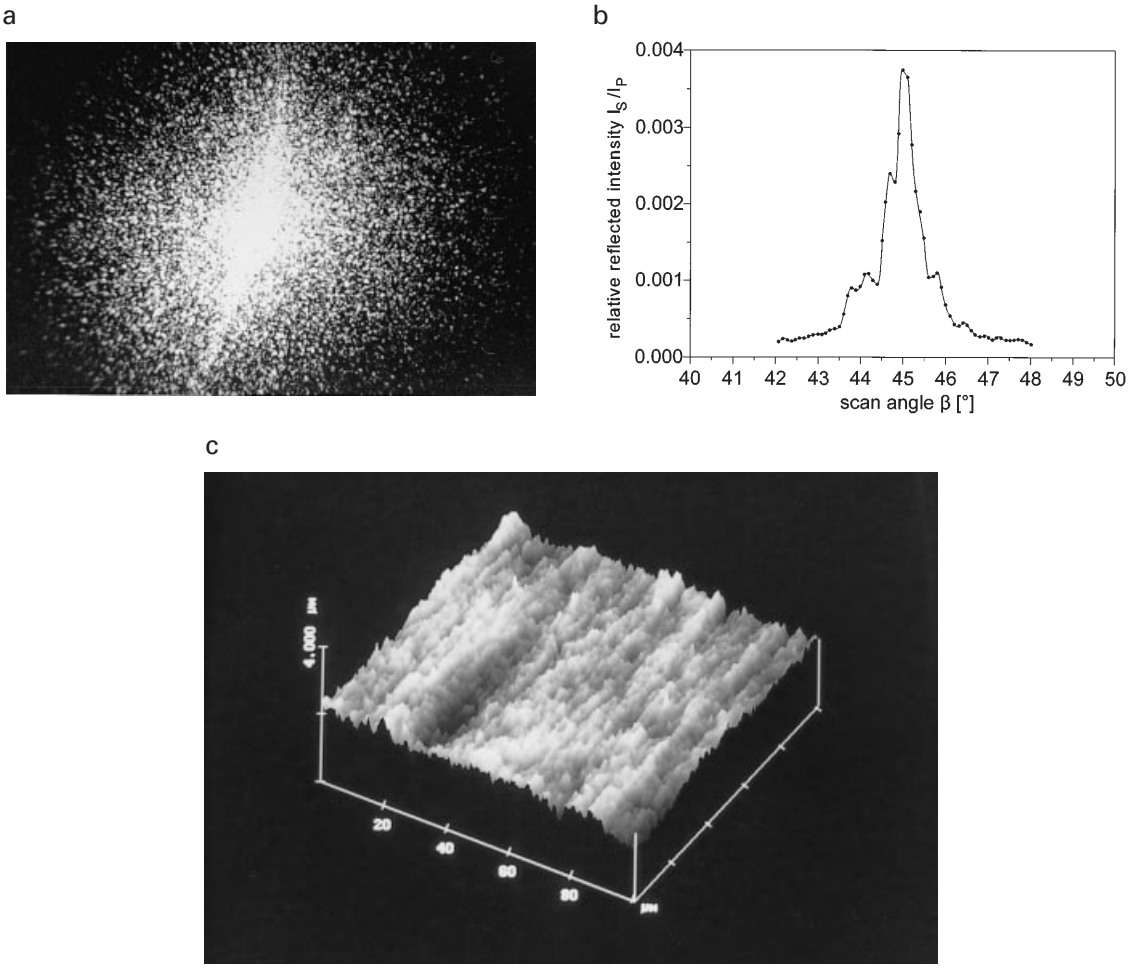

Figure 6 (a) Photograph of the reflected intensity of the β-titanium wire (TMA). The diffuse reflection increased markedly. (b) Scanned distribution of the reflected intensity I_s at an angle of incidence of 45 degrees. (c) A surface scan of 100×100 µm taken by the AFM.

spot of direct reflection for the HIT wire coincides with a narrow peak in the measured angular distribution of reflected intensity (Figure 5a,b). The three-dimensional representation of the surface in Figure 5c gives a realistic impression of a relatively smooth surface with some flat narrow grooves.

Increasing surface roughness is synonymous with an increase in diffuse reflection. The reflection patterns are shown in Figures 6a–8a and the measured angular distribution of the scattered intensity in Figures 6b–8b. A peak of direct reflection can still be identified for the TMA and RMT wires, while the NIT wire produces a nearly uniform distribution of scattered intensity. There is no peak of direct reflection in the speckle pattern or in the measured intensity distribution. The AFM scans of these wires are shown in Figures 6c–8c. They are in good agreement with the profilometric scans. This particularly applies

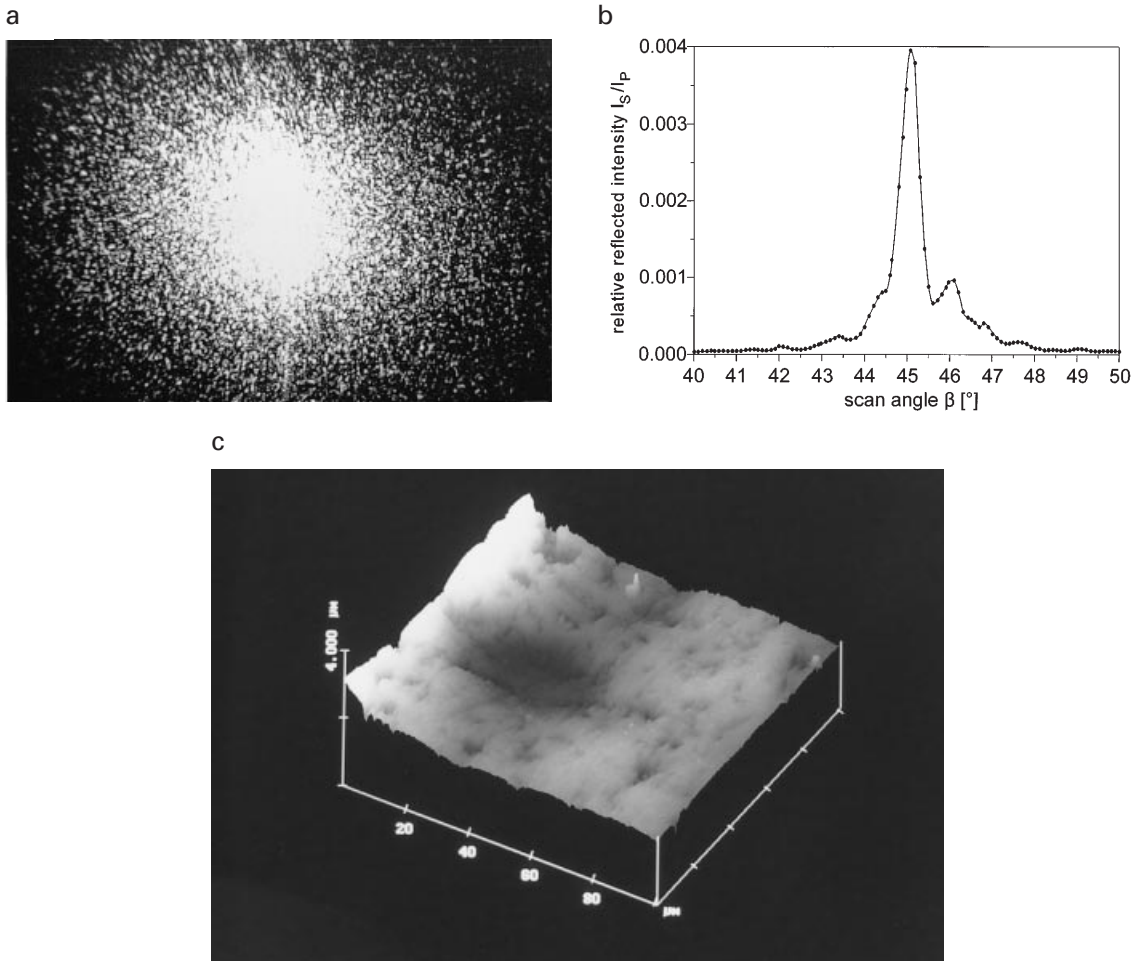

Figure 7 (a) Reflected intensity and (b) spectrum of the nickel-titanium wire (RMT). The direct reflected intensity is decreased further. The AFM picture (c) shows a large variation in surface roughness and a relatively smooth microstructure.

to the RMT wire which has a flat microstructure with deep troughs and high peaks of a large wavelength.

Figure 9 shows the spectrograms of the four wires derived from the measured intensity distributions. The course of the lines corroborates the statement that only relatively smooth surfaces can be measured at grazing incidence with the laser optical method. The data for the very smooth HIT wire are nearly perfectly aligned on a straight line and all values between $\alpha = 70$ and $\alpha = 84$ degrees were used to perform the regression analysis. For all other wires a deviation from the straight line can be observed for angles less than 76 degrees and only the measured relative reflected intensities at angles above this value were included in the regression analysis.

Figure 10a and b summarize the results of the surface roughness measurements for all wires. All orthodontic archwires investigated can

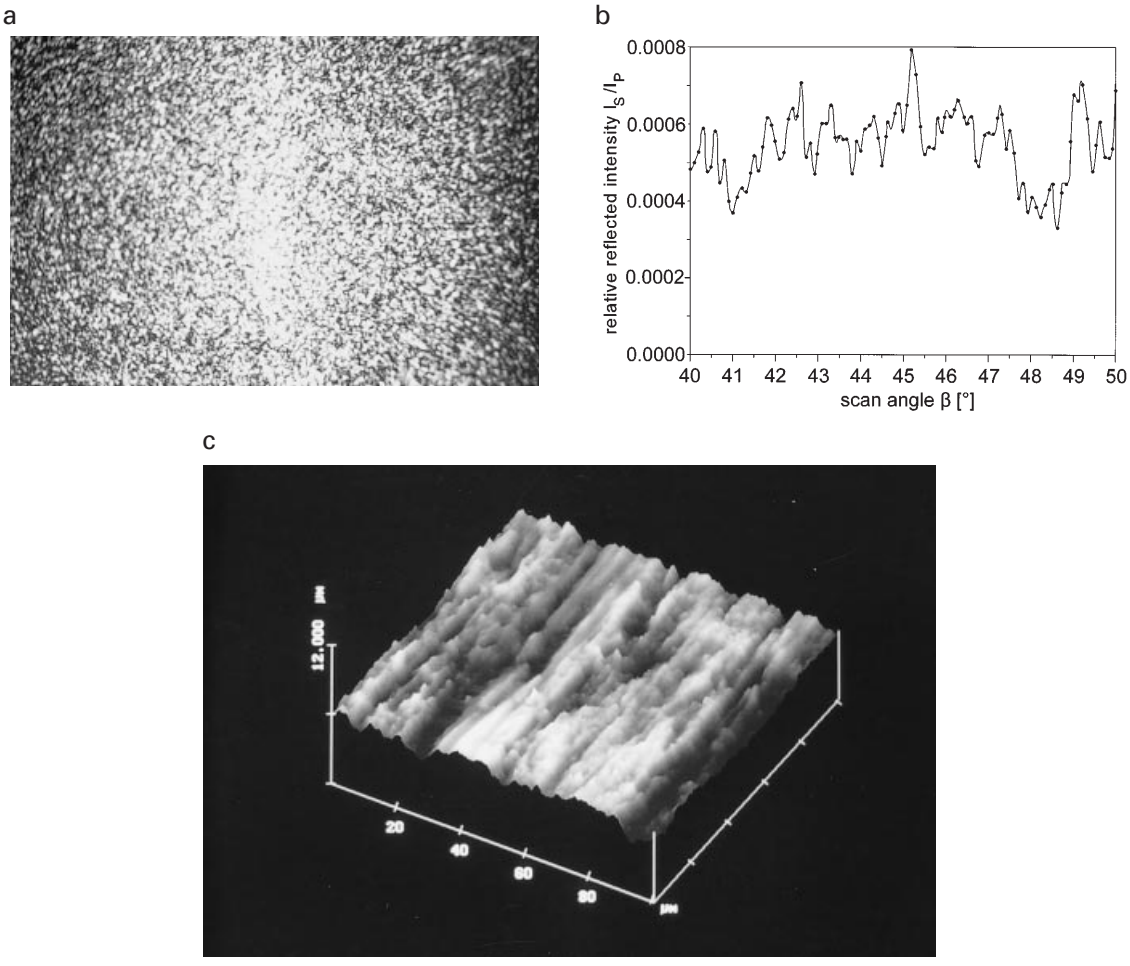

Figure 8 (a) Reflected intensity and (b) spectrum of the nickel-titanium wire (NIT). No direct reflected intensity due to a very high surface roughness. The AFM scan (c) underlines this result. Note the change in the scaling of the *Y*-axis.

be arranged in three groups of different surface quality: smooth ($R_a < 0.2$ µm), medium rough ($R_a < 0.4$ µm), and rough ($R_a > 0.4$ µm). The following products belong to the first group:

HIT ($R_{a,O} \approx 0.10$ µm, $R_a \approx 0.06$ µm, $R_{a,A} \approx 0.09$ µm),
FTS ($R_{a,O} \approx 0.10$ µm, $R_a \approx 0.12$ µm, $R_{a,A} \approx 0.06$ µm),
RMO ($R_a \approx 0.13$ µm, $R_{a,A} \approx 0.12$ µm),
AOT ($R_{a,O} \approx 0.16$ µm, $R_a \approx 0.15$ µm, $R_{a,A} \approx 0.10$ µm),
OSN ($R_{a,O} \approx 0.14$ µm, $R_a \approx 0.17$ µm, $R_{a,A} \approx 0.08$ µm).

The second group of medium rough wires is composed of the products:

ONI ($R_{a,O} \approx 0.19$ µm, $R_a \approx 0.25$ µm, $R_{a,A} \approx 0.17$ µm),
TMA ($R_{a,O} \approx 0.22$ µm, $R_a \approx 0.21$ µm, $R_{a,A} \approx 0.20$ µm),
DNT ($R_{a,O} \approx 0.26$ µm, $R_a \approx 0.16$ µm, $R_{a,A} \approx 0.20$ µm),
RMT ($R_{a,O} \approx 0.27$ µm, $R_a \approx 0.30$ µm, $R_{a,A} \approx 0.35$ µm).

The roughest wires investigated were the products:

NIS ($R_{a,O} \approx 0.44$ µm, $R_a \approx 0.47$ µm, $R_{a,A} \approx 0.40$ µm),
NIT ($R_{a,O} \approx 0.39$ µm, $R_a \approx 0.48$ µm, $R_{a,A} \approx 0.45$ µm),
SSA ($R_{a,O} \approx 0.33$ µm, $R_a \approx 0.57$ µm, $R_{a,A} \approx 0.33$ µm),
NSA ($R_{a,O} \approx 0.31$ µm, $R_a \approx 1.30$ µm, $R_{a,A} \approx 0.89$ µm).

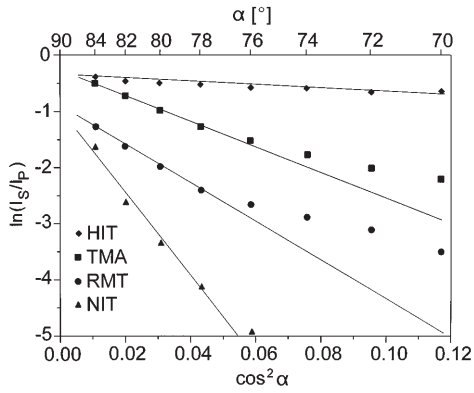

Figure 9 A plot of the log of the relative reflected intensity I_S/I_P for the wires HIT, TMA, RMT, and NIT. As the technique of laser specular reflectance is limited for the roughest surfaces to angles $\alpha \geq 76$ degrees, only these values were used to calculate the optical roughness.

Generally, the correspondence between the results determined with the different methods and for the different batches is in the order of 20 per cent or within the range of the standard deviation. This does not hold for the roughest wires NSA and SSA where the optical measurements established a roughness about 0.30 μm and the profilometric roughness reached values as high as 1.30 μm. As the results for the other wires in the rough group (NIS and NIT) are in a good accordance, this shows that the optical method may be used for the determination of a surface roughness up to 0.50 μm if the angular range in the spectrograms is properly selected.

Discussion

The surface quality of the products investigated differs significantly. A dominant factor determining the surface structure of an orthodontic archwire is the production technique. This hypothesis is confirmed by the fact that the roughness measured for different batches of a certain product is, in most cases, nearly identical. Additionally, in the profilometric as well as in the AFM scans, certain characteristics can be identified that are typical for the surface texture of the wire under investigation. For example, comparison of the scans of the products RMT and NIT show the importance of a final polishing process of the wires. Both RMT and NIT belong to the group of nickel-titanium alloys, but their surface properties differ significantly. While RMT has a very smooth microstructure that can only be achieved by a final polishing, NIT has a very rough surface texture that compares very well to that of the product NIS from the same manufacturer. Similar characteristics could be identified for different batches or other products.

As the production techniques are generally similar for all types of wires from one manufacturer, it is possible to infer that rounded wires of the same brand might have a surface roughness as that observed for their rectangular wires, and each class of alloys may be categorized within the groups smooth, medium rough, and rough.

The roughest wires SSA and NSA are an exception. There are large differences between the results determined with the three methods and for the different cross-sections and tempers. The results for the wire SSA seem to indicate a slight dependence of the surface roughness on the wire cross-section, as the measured roughness decreases with decreasing cross-section for all three methods. However, as the profilometric and AFM roughness also differ significantly for these NiTi wires, this result may be attributed in part to the crystallographic structure of the products. Nickel-titanium alloys exhibit a phase transformation from the martensite (hexagonal closed packed, low temperature phase) to the austenite (cubic centred, high temperature phase) structure at a given transformation temperature (Buehler *et al.*, 1963; Andreasen and Brady, 1972). The alloy composition of the products SSA and NSA is such that this transformation starts between room temperature and the application temperature of 37 degrees (Miura *et al.*, 1986). Concomitant with phase transformation, the surface structure of the wire changes dramatically. A wire that is very smooth in its high temperature phase may change to a very rough one in the low temperature phase. As it was impossible to ensure a constant temperature for all three methods this effect could not be excluded. Further experiments at controlled temperatures for all methods are clearly required.

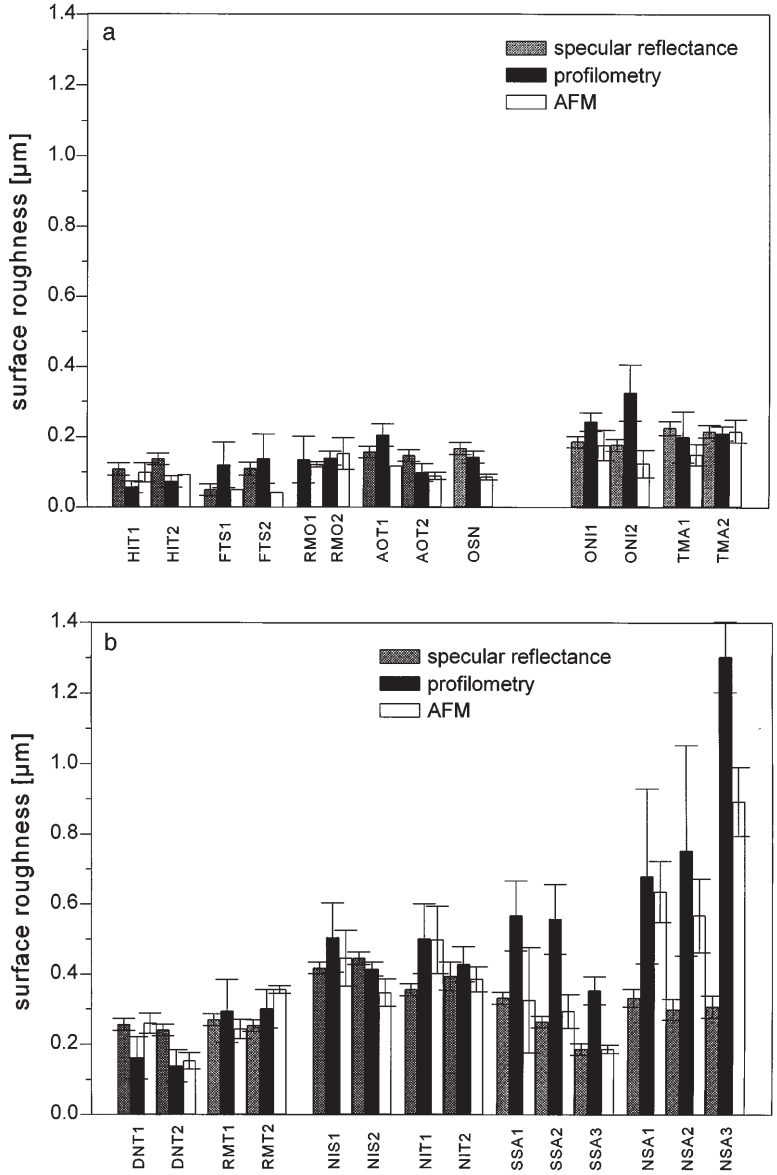

Figure 10 (a,b) Summary of surface roughness values for all products investigated. The correspondence between all three methods is in the range of 20 per cent, except for the wires SSA and NSA. The roughness of these two products is affected by the application temperature, which alters their microstructure and, thus, their external topography.

Comparing the results and the handling of AFM, laser specular reflectance, and profilometry emphasizes the pros and cons of the different methods. Atomic force microscopy is a non-invasive technique delivering three-dimensional realistic impressions of the measured surfaces. It is a very easy and fast method to use, and it is possible to scan nearly the whole wire surface and to analyse subsequently selected areas with prominent characteristics. The roughness is

calculated for these selected areas and it is possible to choose typical regions of the wire surface to characterize a certain product.

The second non-invasive technique, laser specular reflectance, also uses a preselected area of the wire surface. The three-dimensional structure of this area determines the diffuse scattered part of the laser light impinging on the surface and thus the structure of the whole region is used to calculate the roughness of the wire. The drawbacks of the method are an exacting adjustment and the limitation to roughnesses smaller than the wavelength of the laser light used. It is impossible to identify a surface roughness that is beyond this limit and all doubtful cases have to be examined against another method.

The basic difference between both non-invasive techniques and profilometry is that AFM and specular reflectance use a certain region of the wire surface and profilometry uses a single line to determine the surface properties. Scanning multiple lines consecutively would result in a similar surface representation as created by AFM. However, this procedure would be very time consuming and difficult to realize for an orthodontic wire. Additionally, the invasive character of profilometry might damage the scanned surface and falsify the results.

Comparing the results from surface roughness measurements with studies on frictional forces between different orthodontic archwires and brackets (e.g. Drescher *et al.*, 1989; Kusy *et al.*, 1991) shows that the interaction between the different mechanical parameters is rather complex and not yet solved. For example, β-titanium wires generated the highest frictional losses in most investigations. This is in contrast with the results of this study and earlier studies on surface roughness as the β-titanium wires can be arranged in the group of wires with a medium roughness (Kusy *et al.*, 1988; Hartel *et al*., 1992). Consequently, frictional losses cannot directly be deduced from the roughness of a certain orthodontic archwire.

Nevertheless, surface roughness is an essential property of an archwire. Besides the influences on sliding mechanics, surface roughness determines the aesthetics of dental products, as well as the corrosion behaviour and biocompatibility. The extreme variability of the surface roughness of orthodontic NiTi wires suggests that some manufacturers do not pay sufficient attention to the quality of their products.

Address for correspondence

Dr rer. nat. Dipl.-Phys. Christoph Bourauel
Department of Orthodontics
University of Bonn
Welschnonnenstr. 17
D-53111 Bonn
Germany

Acknowledgements

The authors wish to thank Dr Ing. M. Thier, Institute for Materials Research, University of Bochum, for carrying out the EDX analysis of the NiTi wires and 'Minister für Wissenschaft und Forschung, Nordrhein-Westfalen', for financial support.

References

Andreasen G F, Brady P R 1972 A use hypothesis for 55 nitinol wire for orthodontics. Angle Orthodontist 42: 172–177

Bennett H E, Porteus J O 1961 Relation between surface roughness and specular reflectance at normal incidence. Journal of the Optical Society of America 51: 123–129

Bennett J M 1976 Measurement of the rms roughness, autocovariance function and other statistical properties of optical surfaces using a FECO scanning interferometer. Applied Optics 15: 2705–2721

Binnig G, Rohrer H, Gerber C, Weibel E 1982 Tunneling through a controllable vacuum gap. Applied Physics Letters 40: 178–186

Binnig G, Quate C F, Gerber C, 1986 Atomic force microscope. Physical Review Letters 56: 930–933

Buckthal J E, Kusy R P 1988 Effects of cold disinfectants on the mechanical properties and the surface topography of nickel-titanium archwires. American Journal of Orthodontics and Dentofacial Orthopedics 94: 117–122

Buehler W J, Gilfrich J V, Wiley R C 1963 Effect of low-temperature phase changes on the mechanical properties of alloys near composition of TiNi. Journal of Applied Physics 34: 1475–1484

Crane R B 1970 Use of a laser-produced speckle pattern to determine surface roughness. Journal of the Optical Society of America 60: 1658–1663

Drescher D, Bourauel C, Schumacher H A 1989 Frictional forces between bracket and archwire. American Journal of Orthodontics and Dentofacial Orthopedics 96: 397–404

Elson J M, Bennett J M 1979 Relation between the angular dependence of scattering and the statistical properties of optical surfaces. Journal of the Optical Society of America 69: 31–47

Fujii H, Asakura T, Shindo Y 1976 Measurements of surface roughness properties by means of laser speckle techniques. Optics Communications 16: 68–72

Garner L D, Allai W W, Moore B K 1986 A comparison of frictional forces during simulated canine retraction of a continuous edgewise archwire. American Journal of Orthodontics and Dentofacial Orthopedics 90: 199–203

Hartel A, Bourauel C, Drescher D, Schmuth G P F 1992 Die Oberflächenrauheit orthodontischer Drähte—Eine laseroptische und profilometrische Untersuchung. Schweizer Monatsschrift für Zahnmedizin 102: 1195–1202

Haywood V B, Heymann H O, Kusy R P, Whitley J Q, Andreaus S B 1988 Polishing porcelain veneers: an SEM and specular reflectance analysis. Dental Materials 4: 116–121

Hensler D H 1972 Light scattering from fused polycrystalline aluminium oxide surfaces. Applied Optics 11: 2522–2528

Holzer J A, Sung C C 1976 Evaluation of the irradiance of reflected light from rough surfaces. Journal of Applied Physics 47: 3363–3364

Kappert H F, Jonas I, Liebermann M, Rakosi T 1988 Korrosionsverhalten verschiedener orthodontischer Drähte. Fortschritte der Kieferorthopädie 49: 358–367

Keith O, Kusy R P, Whitley J Q 1994 Zirconia brackets: an evaluation of morphology and coefficients of friction. American Journal of Orthodontics and Dentofacial Orthopedics 106: 605–614

Konishi R N, Whitley J Q, Kusy R P 1985 Surface roughness of a dental amalgam via a laser scattering test. Dental Materials 1: 55–57

Kuk Y, Siverman P J 1989 Scanning tunneling microscope instrumentation. Review of Scientific Instrumentation 60: 165–180

Kusy R P, Whitley J Q 1985 *In situ* replication techniques: II. Quantitative methodologies for replicate materials. Journal of Biomedical Materials Research 19: 35–55

Kusy R P, Whitley J Q 1989 Effects of sliding velocity on the coefficients of friction in a model orthodontic system. Dental Materials 5: 235–240

Kusy R P, Whitley J Q, Mayhew M J, Buckthal J E 1988 Surface roughness of orthodontic archwires via laser spectroscopy. Angle Orthodontist 58: 33–45

Kusy R P, Whitley J Q, Prewitt M J 1991 Comparison of the frictional coefficients for selected archwire-bracket slot combinations in the dry and wet states. Angle Orthodontist 61: 293–302

Léger D, Mathieu E, Perrin J C 1975 Optical surface roughness determination using speckle correlation technique. Applied Optics 14: 872–877

Mayhew M J, Kusy R P 1988 Effects of sterilization on the mechanical properties and the surface topography of nickel-titanium archwires. American Journal of Orthodontics and Dentofacial Orthopedics 93: 232–246

Miura F, Mogi M, Ohura Y, Karibe M 1986 The superelastic property of the Japanese NiTi alloy wire for use in orthodontics. American Journal of Orthodontics and Dentofacial Orthopedics 90: 1–10

Peterson L, Spencer R, Andreasen G F 1982 A comparison of friction resistance for nitinol and stainless steel wire in edgewise brackets. Quintessence International 13: 563–571

Sprague R A 1972 Surface roughness measurements using white light speckle. Applied Optics 11: 2811–2816

Tanner L H 1976 The use of laser light in the study of metal surfaces. Optics and Laser Technology 8: 113–116

Tanner L H 1979 A comparison between Talysurf 10 and optical measurements of roughness and surface slope. Wear 57: 81–91

Tanner L H, Fahoum M 1976 A study of the surface parameters of ground and lapped metal surfaces, using specular and diffuse reflection of laser light. Wear 36: 299–316

Vedam K, So S S 1972 Characterisation of real surfaces by ellipsometry. Surface Science 29: 379–395

Vidosic J P 1964 Metal machining and forming technology. Ronald Press, New York

Vorburger T V, Teague E C 1981 Optical techniques for online measurement of surface topography. Precision Engineering 3: 61–83

Whitley J Q, Kusy R P, Mayhew M J, Buckthal J E 1987 Surface roughness of stainless steel and electroformed nickel standards using a HeNe laser. Optics and Laser Technology 19: 189–196

Wickramasinghe H K 1990 Scanning probe microscopy: current status and future trends. Journal of Vacuum Science and Technology A8: 363–368